



UNIVERSITAT
POLITÈCNICA
DE VALÈNCIA



MÁSTER UNIVERSITARIO EN AUTOMÁTICA E INFORMÁTICA INDUSTRIAL

ANEXO : DISEÑO Y CONTROL DE MINITURBIDOSTATOS

AUTOR: FERNANDO NÓBEL SANTOS NAVARRO
TUTOR: ENRIC PICÓ I MARCO
JESÚS ANDRÉS PICÓ I MARCO

CURSO ACADÉMICO: 2016-2017

ÍNDICE ANEXOS

1	Publicación	2
2	Módulo eQEP. Medición de frecuencia.....	11
3	Protocolo de comunicación TCP cliente-servidor	12

1 PUBLICACIÓN

Gracias a los datos experimentales obtenidos en el presente proyecto se ha conseguido realizar una publicación científica en la prestigiosa revista: *“IEEE TRANSACTIONS ON CONTROL SYSTEMS TECHNOLOGY”*.

Output feedback linearization of turbidostats after time scaling

Hernán De Battista, *Member, IEEE*, Enric Picó-Marco, Fernando N. Santos-Navarro, and Jesús Picó, *Senior Member, IEEE*

Abstract—Bioreactors are the workhorses where characterization, scaling-up, and production take place in the biotech and pharma industries. Therefore, feedback control of bioreactors has received much attention in the last years. However, control of bioreactors is difficult due to the uncertain, time-varying and nonlinear nature of the processes involved. In the last years, turbidostats are gaining interest due to the availability of micro- and small-scale devices becoming available for characterization and scaling-up of systems without nutrient limitation. The goal in turbidostats is to keep cell density constant in continuous operation. Thus the control law, i.e. the substrate feeding strategy, must guarantee global or semiglobal convergence to an equilibrium point. In this paper we propose an adaptive control law that globally stabilizes the desired biomass set-point. Further, in some region of the state space the controller linearizes the dynamic behavior after some time scaling. This way, the orbits of the closed loop system are imposed by the designer. The controller implementation only assumes biomass concentration to be measured. Moreover, the intrinsic integral action of the gain adaptation rejects parameter uncertainties. We present both simulated and experimental results showing the performance of the controller as compared with alternative approaches.

Index Terms—Bioreactors; Nonlinear control systems; Output feedback; Adaptive control.

I. INTRODUCTION

INDUSTRIAL biotechnology has traditionally used enhanced and/or genetically modified microorganisms as cell factories to produce specialty metabolites (e.g. amino acids, vitamins, food additives, biofuels,...) of importance for the health, chemical, food and energy sectors among others. Bioreactors of different sizes are the workhorses where characterization, scaling-up, and production take place. Therefore, feedback control of bioreactors has received much attention in the last years. However, control of bioreactors, specially in industrial environments, is difficult due to some characteristics of the processes to be controlled: (i) lack of knowledge on the key variables of the system representing the physiological state of the culture, (ii) high complexity derived from

multi-component non-linear process dynamics, and (iii) large variability. Two key ideas to address model-based design of controllers in this context are the use of simple models based on mass-balances [1], and the development of generic and robust controllers based on the minimal model concept [2]. On the one hand, mass-balance based models constrain the uncertainty in specific terms; the bioreaction kinetics, and the bioreaction yields. On the other, robust controllers based on the minimal model concept use the mass-balance structure and rough information on the kinetics structure and bounds.

Bioreactions can be performed in either batch, fedbatch, or continuous mode. In the later case, the volume of culture inside the bioreactor is kept constant by setting the inlet flow rate equal to the outlet one. The higher risk of contamination and cell mutation in continuous bioreactions have favoured batch and fedbatch ones, leaving continuous ones for processes involving microorganisms with high mutation-stability. Yet continuous bioreactions have some advantages, like increased productivity for biomass and growth associated products, or the possibility to analyze cultures under sets of steady state conditions. Two main classes of continuous bioreactors are mostly used. In chemostats the rate at which fresh medium is continuously added is controlled so as to keep a desired specific growth rate of the microorganism. In the last years, micro- and small-scale turbidostats using a feedback control loop to keep cell density constant are becoming available for characterization and scaling-up of systems without nutrient limitation, and are a promising tool to be used as intermediate step between the lab and the industrial bioreactor [3], [4].

In the case of turbidostats, the control law, i.e. the substrate feeding strategy, must guarantee global or semiglobal convergence to an equilibrium point. To this respect, it can be shown that feeding strategies that are proportional to the reaction rate avoid washout whereas under some extra conditions avoid falling in batch operation. So as to make this control law robust with respect to process uncertainties and variations, and to improve transients, some control strategies discussed in the literature modify it by adapting the controller gain [5], [6] or including error feedback [2], [7]. In the first case, the authors propose adaptive control laws that in the end are integral control ones. Indeed the error appears in the derivative of the feedback gain. A controller that can be applied to regulate biomass, substrate or product concentration in continuous bioprocesses is proposed in [5], whereas a growth rate controller for fedbatch processes is proposed in [6]. These controllers eliminate steady state errors, but they do not improve, even they are prone to deteriorate, the

This work was supported by the National University of La Plata (Project 11-1127), the Agency for the Promotion of Science and Technology ANPCyT (PICT2007-00535) and the National Research Council CONICET (PIP112-200801-01052) of Argentina; and the Spanish government and European Union (FEDER-CICYT DPI2014-55276-C5-1-R). F.N. Santos-Navarro thanks grant BECA-Ai2-UPV. Contact jpico@ai2.upv.es for further questions about this work.

H. De Battista is with the CONICET. LEICI, Facultad de Ingenierías, Universidad Nacional de La Plata, La Plata, Argentina (e-mail: deba@ing.unlp.edu.ar).

E. Picó-Marco, F. N. Santos-Navarro and J. Picó are with the Institut d'Automàtica i Informàtica Industrial, Universitat Politècnica de València, 46022 València, Spain (e-mail: enpimar@isa.upv.es; fersann1@etsid.upv.es; jpico@ai2.upv.es).

transient response. To speed up the transient, a nonlinear proportional controller for the growth rate that results in nonlinear stable dynamics is proposed in [7], but parameter uncertainties cannot be completely rejected and a trade-off appears between robustness and noise. On the other hand, [2] presents a nonlinear proportional control with adaptive gain, leading to a class of nonlinear PI controller. Although this controller exhibits fast convergence properties and robustness, it is not clear how to impose the desired dynamics and care should be taken to avoid controller saturation.

In this paper we propose an adaptive control law that globally stabilizes the desired biomass set-point. Further, in some region of the state space the controller linearizes the dynamic behavior after some time scaling. This way, the orbits of the closed loop system are imposed by the designer. The controller implementation assumes biomass concentration is measured. From this measurement, the reaction rate can be estimated using high-gain or sliding observers [8], [9]. The intrinsic integral action of the gain adaptation rejects parameter uncertainties. If, conversely, the reaction rate is indirectly measured or calculated and some error appears, then the controller is not completely capable of rejecting the steady state error. In that case, the error is bounded.

The paper is organized as follows. In Section II the problem is formulated. The proposed control law and its analysis is considered in Section III and Section IV respectively. Some simulations highlighting the performance of the devised controller are shown in Section V. The experimental validation is shown in Section VI. Finally, Section VII outlines the conclusions of the work.

II. PROBLEM STATEMENT

Let consider the mass balance equation of a pure culture growing under a single carbon and energy source (CES) being continuously fed to the reactor.

$$\begin{aligned} \dot{x} &= \mu(x, s)x - D(t)x \\ \dot{s} &= -y\mu(x, s)x + D(t)(s_i - s) \end{aligned} \quad (1)$$

where $x \in \mathbb{R}_+$ is the biomass concentration, $s \in \mathbb{R}_+$ the substrate concentration (CES), $s_i \in \mathbb{R}_+$ the substrate concentration in the inlet flow, $\mu(x, s)$ the specific growth rate, y the substrate-biomass conversion yield, and $D(t)$ the dilution rate, i.e. the ratio between the flow rate and the culture volume, that will be used as control input.

Assumption 2.1: We will assume that the specific growth rate is continuously differentiable ($\mu(x, s) \in \mathcal{C}^1$), vanishes if there is no substrate ($\mu(x, 0) \equiv 0$), it is strictly positive whenever there is available substrate ($\mu(x, s) > 0 \quad \forall s > 0$), and it is bounded ($\mu(x, s) \leq \mu_m \quad \forall x, s \geq 0$). These are sensible assumptions fulfilled by all standard specific growth rate models [1].

Assumption 2.2: We will assume that the dilution rate is nonnegative and bounded so that $0 \leq D(t) \leq \bar{D} \quad \forall t$. Note that unbounded dilution rates make no sense from a bioprocess physical viewpoint. Negative dilution rates would imply emptying the bioreactor.

Assumption 2.3: Assume biomass concentration x is available for measurement.

Definition 2.1: A bioprocess operates in continuous mode when there exists $T_c \geq 0$ such that $D(t) \geq d > 0 \quad \forall t \geq T_c$, for some sufficiently small d .

The goal is to design a control law $D(t)$ that globally stabilizes system (1) at the specified biomass set-point x^* .

III. PROPOSED CONTROL LAW

A. Growth rate proportional feeding laws

As mentioned in section I, a family of controllers of the form

$$D(x, \mu) = \gamma \mu x \quad (2)$$

have been proposed in the literature, mainly for substrate or growth regulation. Although many of them have been originally devised for fed-batch processes, they can also be applied to continuous ones.

Using (2), the closed loop dynamics can be expressed as:

$$\begin{aligned} \dot{x} &= D(x, \mu)(\gamma^{-1} - x) \\ \dot{s} &= D(x, \mu)(s_i - y\gamma^{-1} - s) \end{aligned} \quad (3)$$

Let us consider the simplest case in which $\gamma = 1/x^*$, and x^* is the set-point for biomass. Then:

$$\begin{aligned} \dot{x} &= D(x, \mu)(x^* - x) \\ \dot{s} &= D(x, \mu)(s^* - s) \end{aligned} \quad (4)$$

where $s^* = s_i - yx^*$ is the substrate equilibrium point.

It is clear that for a continuous bioreaction as stated in Definition 2.1, this controller locally stabilizes the equilibrium $P^* = (x^*, s^*)$. The controller decouples the dynamics of both concentrations, which converge to their steady state values at the same rate.

The idea now is to semiglobally stabilize the biomass concentration preserving the control law structure (2), i.e. to feed the reactor in proportion to growth rate, but changing the feedback gain γ so as to improve the transient dynamics. The ultimate objective is to linearize, at least locally, the output dynamics, thus providing some tools to tune the controller in terms of the desired response shape.

B. Adaptive shaping of γ

Recall that $\gamma = 1/x^*$ will locally stabilize the equilibrium $P^* = (x^*, s^*)$. The goal now is to shape γ so as to improve convergence of x towards the desired set-point x^* . To this end, we propose the following control adaptive control law.

Theorem 3.1: Let the system (1), and x^* the desired set-point for biomass concentration. Let f be a function satisfying

$$\begin{aligned} f &\in \mathcal{C}^0 \\ f(\gamma) &> 0 \quad \forall \gamma \in (\underline{\gamma}, \bar{\gamma}), \quad \frac{y}{s_i} < \underline{\gamma} < \gamma^* < \bar{\gamma} \\ f(\underline{\gamma}) &= 0 \\ f(\bar{\gamma}) &\xrightarrow{\bar{\gamma} \rightarrow \infty} 0 \\ f(\gamma) &= 1 \quad \forall \gamma \in \Gamma = [\gamma_m, \gamma_M] \subset (\underline{\gamma}, \bar{\gamma}), \quad \gamma^* \in \Gamma \end{aligned} \quad (5)$$

with $\gamma^* = \frac{1}{x^*}$. Then, the controller

$$\begin{aligned} D(\mu, x) &= \gamma \mu x \\ \dot{\gamma} &= -\gamma^2 [(\mu - D)x(1 - a) - Db(x - x^*)] f(\gamma) \\ \gamma_0 &\in (\underline{\gamma}, \bar{\gamma}) \end{aligned} \quad (6)$$

with $b > (a - 1) > 0$:

- a) globally stabilizes biomass at x^* , and
- b) linearizes the biomass dynamics in a transformed time scale when the controller enters the set Γ .

C. Time scaling

In order to prove Theorem 3.1, it is convenient to express the closed loop dynamics in a new time scale τ . To that end, consider the time scaling given by:

$$d\tau = D(x, \mu)dt \quad (7)$$

Now, defining the time derivative w.r.t. the new time variable as $(\cdot)' = \frac{d(\cdot)}{d\tau}$, the closed loop dynamics (3) become:

$$\begin{aligned} x' &= \gamma^{-1} - x \\ s' &= s_i - y\gamma^{-1} - s \end{aligned} \quad (8)$$

Notice that the system in the transformed time scale has its eigenvalues at -1 . One can also see that γ can be shaped to improve convergence of one variable, say x , relative to the other. Notice again that the dynamics of biomass and substrate are also decoupled in the transformed time-scale. Therefore, one may analyze partial stability of the system with respect to one of the states independently of the other.

Theorem 3.2: The time scaling (7) defines a stability preserving map.

Proof Taking into account Assumption 2.2, and assuming continuous mode operation, the time-scaling (7) defines a strictly increasing and onto function $\xi : t \rightarrow \tau$. Thus, the homomorphism given by the identity transformation for the coordinates and the time-scaling defined by (7) preserves stability. See Th. 7 and Coroll. 8 in [8]. \square

D. Proof of Theorem 3.1

Assume for the time being that the control law (6) induces a well defined time scaling (7).

Applying the time scale transformation, and taking into account the dynamics (8), the control law (6) in the transformed τ -time scale becomes:

$$\begin{aligned} D(\mu, x) &= \gamma\mu x \\ \gamma' &= -\gamma^2 [(\gamma^{-1} - x)(1 - a) - b(x - x^*)] f(\gamma) \end{aligned} \quad (9)$$

First we prove partial global stability of the closed loop system corresponding to the biomass dynamics. Recall that $\gamma^* = (x^*)^{-1}$. Define the errors:

$$\begin{aligned} \tilde{x} &= x - x^* \\ \tilde{\gamma} &= \gamma^{-1} - \gamma^{*-1} \end{aligned} \quad (10)$$

Taking derivative w.r.t. τ we obtain the error dynamics

$$\begin{aligned} \tilde{x}' &= \tilde{\gamma} - \tilde{x} \\ \tilde{\gamma}' &= f(\gamma) [(\tilde{\gamma} - \tilde{x})(1 - a) - b\tilde{x}] \end{aligned} \quad (11)$$

Let us now define the following positive definite radially unbounded function:

$$\begin{aligned} W_1 &= \int_0^{\tilde{\gamma}} \frac{g}{f(\frac{\gamma^*}{1+g\gamma^*})} dg \\ W_2 &= \frac{b-a+1}{2} \tilde{x}^2 \\ W &= W_1 + W_2 \end{aligned} \quad (12)$$

with $b - a + 1 > 0$. Using the Leibnitz Integral Rule for W_1 , the τ -time derivative of (12) along the state trajectory is:

$$\begin{aligned} W_1' &= \frac{\tilde{\gamma}\tilde{\gamma}'}{f(\gamma)} = -(a-1)\tilde{\gamma}^2 - (b-a+1)\tilde{\gamma}\tilde{x} \\ W_2' &= -(b-a+1)\tilde{x}^2 + (b-a+1)\tilde{\gamma}\tilde{x} \\ W' &= -(a-1)\tilde{\gamma}^2 - (b-a+1)\tilde{x}^2 \end{aligned} \quad (13)$$

which is negative definite for $a > 1$. Therefore, the equilibrium $(\tilde{x}, \tilde{\gamma}) = (0, 0)$ of the error dynamics (11) is globally asymptotically stable.

From Theorem 3.2, the time scaling (7) defines a stability preserving map. Consequently, the closed loop defined by the biomass dynamics in (1) and the controller (5)-(6) in the (x, t) -coordinates is asymptotically stable if and only if the closed loop biomass dynamics (8)-(5)-(9) in the (x, τ) -coordinates is.

Next we show that, after some finite time T_c , the control law (6) linearizes the biomass dynamics in the transformed time scale, within a set $\Gamma = [\gamma_m, \gamma_M]$. To this end, differentiating x in (8) twice w.r.t. τ , one gets

$$\begin{aligned} x'' &= -\gamma^{-2}\gamma' - x' \\ &= f(\gamma) [x'(1-a) - b(x-x^*)] - x' \end{aligned} \quad (14)$$

Since $\tilde{\gamma}$ asymptotically converges to zero, there will exist some finite time T_c such that $\gamma \in \Gamma$ for all $\tau \geq T_c$ where, from (5), $f(\gamma) = 1$. Therefore, once γ enters the set Γ the system will behave according to the linearised dynamics:

$$x'' + ax' + b(x - x^*) = 0 \quad (15)$$

Remark 3.1: Notice that although in this linear region in the transformed τ time scale it suffices to choose $a, b > 0$ to ensure asymptotic stability, the Lyapunov function (12) we found is more restrictive.

Now we are in position to see that the time scaling (7) is well defined. To this end, it suffices to see that the dilution rate $D(\mu, x)$ in (6) is bounded and strictly positive, so that Theorem 3.2 can be invoked. That is, we must prove that the control law (5)-(6) induces continuous mode operation.

From Theorem 3.1, the adaptation gain γ will be bounded, with $\gamma(t) \in (\underline{\gamma}, \bar{\gamma}) \quad \forall t \geq t_0$. Also biomass x will be bounded. Finally, Assumption 2.1 ensures that the specific growth rate μ is bounded. Thus, from boundedness of γ , μ and x we conclude that of the dilution rate $D(\mu, x)$.

Next we will prove that $D(\mu, x)$ does not vanish. To this end, recalling that $\gamma(t) \in (\underline{\gamma}, \bar{\gamma}) \quad \forall t \geq t_0$, it will suffice to prove that both the biomass x and the specific growth rate μ are bounded away from zero. That is, we must prove that the control law avoids both washout of biomass and batch operation with substrate depletion.

The point $x = 0$ is a stable fixed point of system (1) which corresponds to biomass washout. We can assume initial conditions satisfying $x_0 > 0$, i.e. there is some initial biomass concentration in the bioreactor. From Theorem 3.1, x^* is an asymptotically stable equilibrium point for biomass. Therefore, there will exist some sufficiently small $0 < \underline{x} < x^*$ such

that the region $R_{\bar{x}} = \{(x, s) | x \geq \bar{x}\}$ is positively invariant. That is, the control law (5)-(6) avoids washout.

Now, given the properties for the specific growth rate in Assumption 2.1 and the result above, to prove that the specific growth rate $\mu(x, s)$ does not vanish it suffices to prove that the substrate concentration s so does not. Notice that every point in $\mathcal{S} = \{(x, s) | s = 0\}$ is a marginally stable fixed point of the autonomous system resulting from setting $D(t) \equiv 0$ in (1). So, we must require \mathcal{S} not to be locally attractive.

Lemma 3.1: \mathcal{S} is not locally attractive iff

$$\lim_{s \rightarrow 0^+} D(x, s) > yx \lim_{s \rightarrow 0^+} \frac{\mu(x, s)}{s_i - s} \quad \forall x \in [\underline{x}, \bar{x}] \quad (16)$$

Proof By continuity, if $D(x, s)$ fulfills (16), then there exists s sufficiently small such that $\forall x \in [\underline{x}, \bar{x}]$ the dilution rate verifies $D(x, s) \geq \frac{yx\mu(x, s)}{s_i - s}$ and, consequently, the substrate concentration in system (1) will increase. Therefore, the region

$$R_{\bar{s}} = \{(x, s) | s \geq \bar{s}\} \quad (17)$$

is positively invariant. On the other hand, if \mathcal{S} is not locally attractive then from the second equation in (1) the inequality (16) holds.

That is, if we do not want to converge to \mathcal{S} , then D cannot go to zero faster than the reaction rate μx . Now, notice the control law (6) fulfills Lemma 3.1 provided $\underline{\gamma} > \frac{y}{s_i}$. Therefore, the specific growth rate $\mu(x, s)$ is bounded away from zero.

Remark 3.2: Notice that the inequality $\underline{\gamma} > \frac{y}{s_i}$ implies that the desired set-point for biomass concentration must be bounded by $x^* < \frac{s_i}{y}$. This is sensible, as it simply says that at equilibrium the amount of CES converted into biomass (yx^*) must be less than the one in the input flow (s_i).

Thus, we have proved that both the biomass x and the specific growth rate $\mu(x, s)$ are bounded from above, and bounded away from zero. Therefore, the time scaling (7) is well defined.

On the other hand, D vanishes on \mathcal{S} . Therefore, this class of controller is not able to start the process from $s = 0$. Anyway, the non-attractiveness condition (16) is always satisfied since $x^* < \frac{s_i}{y}$. Thus, this controller (semi)globally stabilizes the equilibrium.

This completes the proof of Theorem 3.1.

IV. CONTROLLER PERFORMANCE

A. Closed loop poles in the τ time-scale

Recall that after some finite time, the biomass error in the transformed time-scale τ will follow the linear dynamics (15). By choosing a, b in the control law (6), and using $b - a + 1 > 0$, we can place the corresponding eigenvalues λ_1, λ_2 of the closed-loop system with:

$$\begin{aligned} \omega_0 &= \sqrt{\lambda_1 \lambda_2} = \sqrt{b} \\ \xi &= \frac{\lambda_1 + \lambda_2}{2\omega_0} = \frac{a}{2\sqrt{b}} \\ \frac{1}{2}\omega_0^{-1} < \xi < \frac{1}{2}(\omega_0 + \omega_0^{-1}) \end{aligned} \quad (18)$$

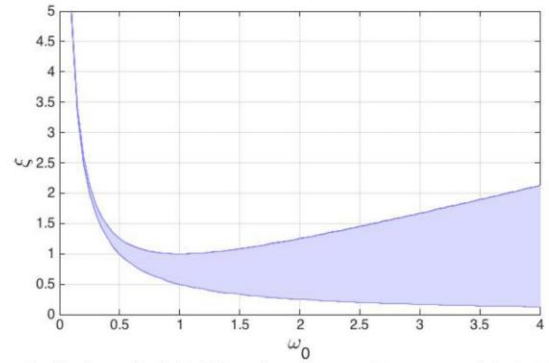


Figure 1. Region of admissible values for ω_0, ξ to ensure global stability

where ω_0 is the natural frequency, ξ the damping coefficient. The values (ω_0, ξ) should be selected to fall within the region shown in figure Fig. IV-A.

B. Effects of the growth rate observer

Any measurement error in x will produce an error in the steady state. Yet, the proposed controller can be tuned so as to significantly reduce the error. To analyze the controller performance, we consider the case that estimation of μ does introduce an error, so that the estimated specific growth rate $\hat{\mu}$ is $\hat{\mu} = \mu + \delta_\mu$, with $\delta_\mu = \frac{(\mu - \hat{\mu})}{\hat{\mu}}$. Now consider the controller (6) using the estimated value $\hat{\mu}$. Replacing $\hat{\mu}$ for μ in (6) gives:

$$\dot{\gamma} = -\gamma^2(-\dot{x}(a-1) + (\delta_\mu \mu x(a-1)) - Db(x-x^*))f(\gamma) \quad (19)$$

that in the transformed time scale results in:

$$\begin{aligned} x' &= ((1 - \delta_\mu)\gamma)^{-1} - x \\ \gamma' &= -\gamma^2 f(\gamma)(x'(1-a) - b(x-x^* - \frac{\delta_\mu(a-1)}{(1-\delta_\mu)\gamma b})) \end{aligned} \quad (20)$$

At steady state, $(1 - \delta_\mu)\gamma_{ss}x_{ss} = 1$, and $x_{ss} = x^* - \frac{\delta_\mu(a-1)}{(1-\delta_\mu)\gamma_{ss}b}$. Therefore:

$$x_{ss} = \frac{x^*}{1 - \delta_\mu \frac{(a-1)}{b}} \quad (21)$$

Defining $\delta_{x^*} = \frac{x_{ss} - x^*}{x^*}$, leads to:

$$\delta_{x^*} \cong \delta_\mu \frac{(a-1)}{b} \quad (22)$$

We can define the error gain as:

$$\Delta_{x/\mu} := \frac{\delta_{x^*}}{\delta_\mu} \cong \frac{(a-1)}{b} \quad (23)$$

Recall that $b > a - 1 > 0$. Notice $\Delta_{x/\mu} \rightarrow 0$ as $a \rightarrow 1$. Therefore, there is a compromise between transient response (speed and overshoot) and steady state error. If we design a, b to have a given ξ and damping factor $\sigma = a/2$ (notice σ will define the settling time), then

$$\Delta_{x/\mu} \cong \frac{(2\sigma - 1)\xi}{\sigma^2} \quad (24)$$

For a given damping coefficient ξ , the error has a single local maximum $\Delta_{x/\mu, \max} = \xi$ at $\sigma = 1$ ($a = 2$) and goes to zero

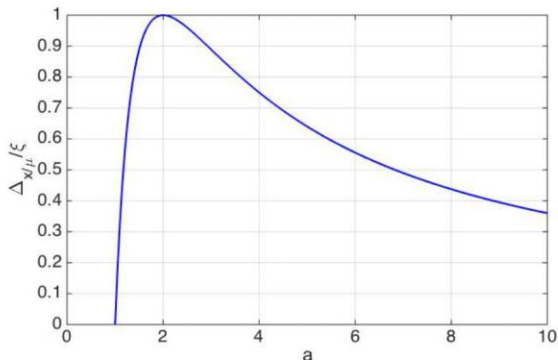


Figure 2. Ratio of steady state regulation error to μ estimation error of the proposed algorithm (normalised w.r.t. ξ)

as $a \rightarrow 1$ or $a \rightarrow \infty$ (see figure 2). Also, the smaller ξ , the smaller the error will be.

The steady state error of the classical algorithm (2) is very similar to the error in the estimation of μ : $\Delta_{x/\mu} \cong 1$. If well designed, the proposed controller will significantly reduce the error. Anyway, to avoid this source of error one can estimate μ using a supertwisting observer that gives finite time convergence with zero steady state estimation error.

V. SIMULATED RESULTS

Since the time scaling (7) is a regular transformation, the relationship between t and τ is monotonous. This means that all properties independent of time, e.g. overshoot, will be preserved by the time scaling, and those depending on time will preserve order, provided the initial conditions are the same. Preservation of magnitude and order is a key characteristic that makes tuning of the proposed algorithm more simple than existing alternatives. There is a direct mapping between changes in the controller parameters a , b , and its effect on the closed loop time response.

Figure 3 shows the biomass concentration x in the original time scale t and modified one τ for different values of the parameters a, b in the proposed algorithm, chosen so that the damping factor keeps the same. Notice all three solutions in figure 3 have the same settling time, for they share the same damping factor σ . Figure 4 shows how time scaling preserves order. That is, slower time responses in the τ scale will correspond to slower ones in the t time-scale. Notice the overshoot is conserved in the transformation, but it is not exactly the same in all cases, in spite of having a common damping coefficient $\xi = 0.5$. The small differences are due to the fact that linearization in the τ time-scale is achieved after a transient, that may be slightly different in each case. On the other hand, the controller performance is very robust with respect to variability in the substrate initial conditions, as shown in Figure 5. This is due to the fact that the transient response of the linearised dynamics in the transformed time scale does not depend on the initial substrate conditions. Only the nonlinear short transient to reach the linearised region affects. Therefore, only the dependence of the time-scaling on the substrate s -via the specific growth rate $\mu(x, s)$ - to get back into the original time scale t will induce differences. In

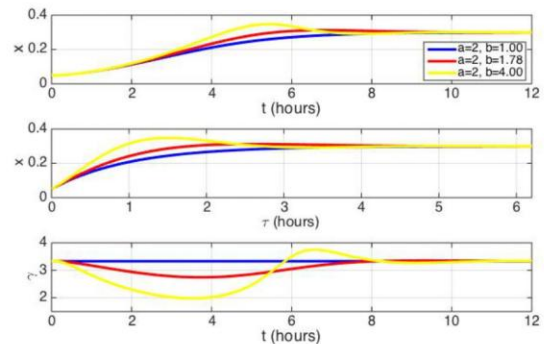


Figure 3. Biomass concentration x in the original time scale t (top) and modified one τ (middle), and adaptation gain γ (bottom) for the proposed algorithm and values of ξ : 1 (blue), 0.75 (red), 0.5 (yellow). In all cases $\sigma = 2$. Initial conditions: $(x_0, s_0) = (0.05, 0.001)$, set-point $x^* = 0.3$.

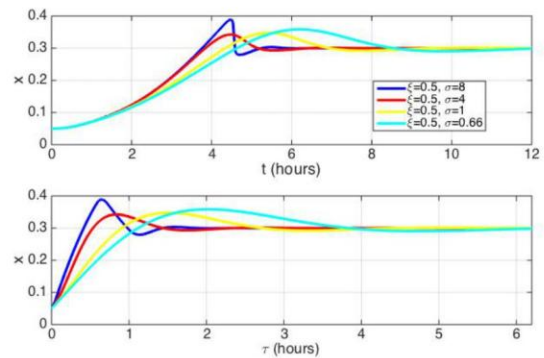


Figure 4. Biomass concentration x in the original time scale t (top) and modified one τ (bottom) for the proposed algorithm and common damping coefficient $\xi = 0.5$. The damping factors are $\sigma = 8$ (blue), $\sigma = 4$ (red), $\sigma = 2$ (yellow), and $\sigma = 1$ (cyan). Initial conditions: $(x_0, s_0) = (0.05, 0.001)$, set-point $x^* = 0.3$.

practice, the biorreaction operates most of the time at values of substrate driving $\mu(x, s)$ close to saturation. Under this situation, the sensitivity of $\mu(x, s)$ w.r.t. s is very small for the standard specific growth rate functions –e.g. Monod. This explains the robustness with respect to the substrate initial conditions observed in Figure 5.

Next we compare the proposed controller both with the baseline controller (2) and with the one proposed in [5]:

$$\begin{aligned} \dot{\gamma} &= K\mu x(x - x^*)(\gamma - \underline{\gamma})(\bar{\gamma} - \gamma) \quad \gamma_0 \in (\underline{\gamma}, \bar{\gamma}) \\ D(\mu, x) &= \gamma\mu x \end{aligned} \quad (25)$$

Notice the controller (25) consists basically of the baseline controller where the gain γ is adapted, introducing an integral compensation. Differing from our proposal, the controller developed in [5] does not include proportional action, thus limiting the achievable controller performance. Additionally, it does not exhibit a linear region in any time scale, so it is not so easy to tune the gain K .

Figure 6 shows the time t evolution of the biomass concentration, dilution rate, and adaptation gain for the proposed controller and the baseline controller (2). Notice with the proposed controller one can achieve better settling time, and can easily set the desired transient specifications.

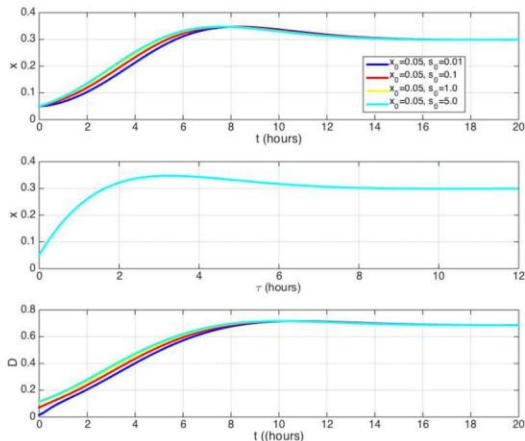


Figure 5. Biomass concentration x in the original time scale t (top) and modified one τ (bottom) for the proposed algorithm for different substrate initial conditions. Initial conditions: $(x_0, s_0) = (0.05, 0.001)$ (blue), $(x_0, s_0) = (0.05, 0.001)$ (red), $(x_0, s_0) = (0.05, 0.001)$ (yellow). Parameters: $(a, b) = (2, 4)$. Set-point $x^* = 0.3$.

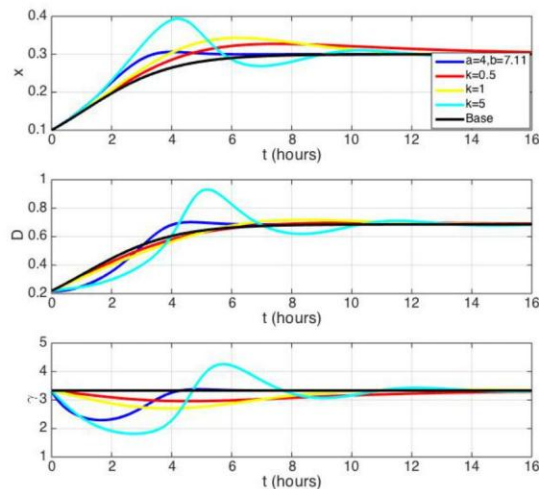


Figure 7. Biomass concentration x (top) dilution rate D (middle) and gain γ (bottom). Initial conditions: $(x_0, s_0) = (0.1, 1.0)$. Set-point $x^* = 0.3$. Proposed controller: $(a, b) = (4, 7.11)$ (blue). Controller (25): $K = 0.5$ (red), $K = 1$ (yellow), $K = 5$ (cyan). Baseline controller (black).

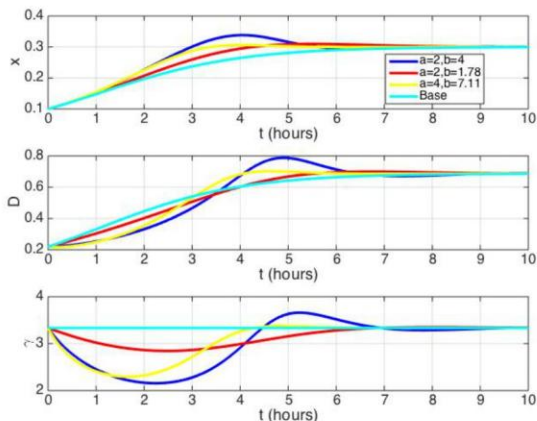


Figure 6. Biomass concentration x (top) dilution rate D (middle) and gain γ (bottom) for the proposed algorithm and the base one. Initial conditions: $(x_0, s_0) = (0.1, 1.0)$. Set-point $x^* = 0.3$. Parameters: $(a, b) = (2, 4)$ (blue), $(a, b) = (2, 1.78)$ (red), $(a, b) = (4, 7.11)$ (yellow), baseline controller (cyan).

On the other hand, the controller (25) does not improve the transient response of the classical controller, as shown in Figure 7. Its inherent integral action can be useful to reject uncertainties in the calculation/measurement of μ or μx . Note that for small values of gain k the nominal response of this controller is practically not altered with respect to that of the baseline controller. However, as k increases, the gain γ is adapted as response to the error and then it takes a long time to recover its steady state value. For even higher values of k , the nominal response is seriously degraded by the presence of large overshoots that can be attributed to a too strong integral action.

Finally, let us compare the response of the controllers in the presence of μ estimation error. The problem of pure integral adaptive controllers, as (25), is that a large integral action that drives the error to zero reasonably fast deteriorates

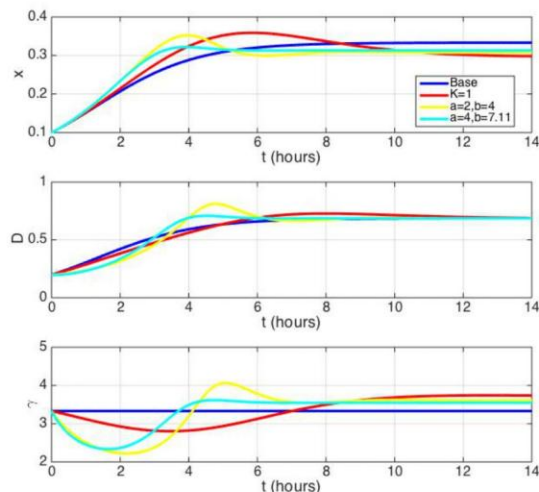


Figure 8. Steady state error. Biomass concentration x (top) dilution rate D (middle) and gain γ (bottom). Initial conditions: $(x_0, s_0) = (0.1, 1.0)$. Set-point $x^* = 0.3$. Proposed controller: $(a, b) = (4, 7.11)$ (blue). Controller (25): $K = 0.5$ (red), $K = 1$ (yellow), $K = 5$ (cyan). Baseline controller (black).

significantly the transient response. In figure 8 we show the response when the growth rate is estimated with a -10% error. The classical controller, the proposed controller for a pair of settings and the controller (25) for its optimal gain are compared. Although controller (25) response in the large tends to the desired value, the transient is much longer (12 hours) than the one obtained with our controller (5 hours).

VI. EXPERIMENTAL RESULTS

We used the experimental setup shown in Fig. 9. It consists of a 16ml turbidostat adapted from [4] and fed by a syringe pump (NE-1000, New Era Pump Systems, Inc.). Volume was



Figure 9. Experimental turbidostat setup.

kept constant by injecting pressurized air using a small pump. Optical density at 650 nm (OD_{650}) was measured using an absorbance custom-made sensor using a photodiode converting light intensity to frequency (TSL235-LF, Farnell). In our working range there is a linear relationship between OD_{650} and biomass concentration, so we controlled optical density. We grew *E. coli* transformed cells containing the blue-purple chromoprotein amilCP using SOB medium as substrate with 20mM glucose (3.603 g/L).

To estimate the specific growth rate μ from biomass measurements we used the super-twisting based observer for continuous bioreactions in [10] tuned using the methodology in [8]. This observer converges in finite time. In all cases we set the same initial condition $\mu(0) = 0.25$ for the estimated specific growth rate. We did not allow for an initial open loop period for the observer to converge before closing the loop. In all cases the observer converged in less than one hour.

Fig. 10 and Fig. 11 show the experimental results obtained fit well with the theoretical predictions considering the noisy, uncertain and time-varying context. We used the parameters $(a, b) = (4, 7.11)$ corresponding to a peak time of $t_p = 1.8$ hours, settling time of $t_s = 4$ hours (98% criterium) and overshoot $\delta = 0.16$, and $(a, b) = (2, 4)$ yielding $t_p \approx 1.8$ hours, $t_s = 2$ hours and $\delta = 0.03$. The proposed control law achieves faster convergence to the set point than the baseline controller with the specified transient characteristics (Fig. 10). Notice the controller is robust with respect to uncertain factors that affect the specific growth rate and may differ from one experiment to another (e.g. substrate initial concentration, oxygen diffusion, cells metabolic state, etc.) As showed in Fig. 10 (bottom) the time responses in the τ and t time scales preserve order and magnitude.

VII. CONCLUSION

In this work we have proposed an adaptive control law that globally stabilizes the desired biomass set-point in continuous bioreactions. Using time scaling we render the system linear in the transformed time scale, where analysis and tuning of the controller becomes extremely simple. Stability is preserved in the original time domain, along with important time-response characteristics as order and magnitude relationships. Furthermore, our controller only assumes biomass concentration is

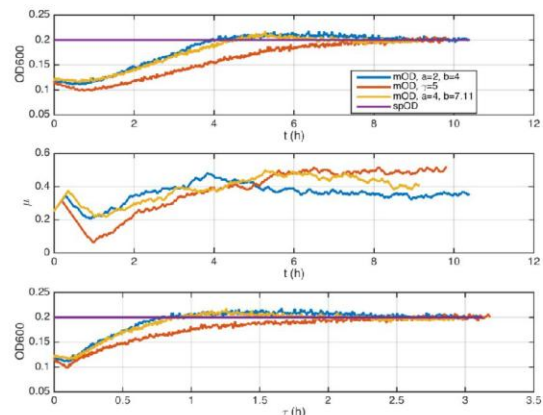


Figure 10. Biomass concentration x (top), estimated specific growth rate μ (mid), and biomass concentration x in the transformed τ -time (bottom). Initial conditions: $x_0 \approx 0.12$. Set-point $x^* = 0.2$. Proposed controller: $(a, b) = (4, 7.11)$ (yellow), $(a, b) = (2, 4)$ (blue). Baseline controller (orange).

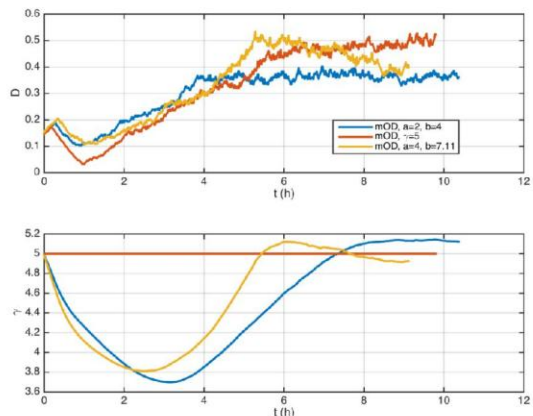


Figure 11. Dilution D (top) and controller gain γ (bottom). Initial conditions: $x_0 \approx 0.12$. Set-point $x^* = 0.2$. Proposed controller: $(a, b) = (4, 7.11)$ (yellow), $(a, b) = (2, 4)$ (blue). Baseline controller (orange).

measured, and does not require a detailed model of the growth kinetics or knowledge of the bioreaction yields. The intrinsic integral action of the gain adaptation rejects parameter uncertainties. If, conversely, the reaction rate is indirectly measured or calculated and some error appears, then the controller is not completely capable of rejecting the steady state error. In that case, the error is bounded. Yet, the proposed controller can be tuned so as to significantly reduce the error.

Notice alternative stability preserving maps could have been used including both time scaling and coordinates transformation (e.g. $d\tau = \mu dt$ with $x = 1/z$). This opens the possibility to design controllers with slightly different transient time-deformation characteristics when changing between the time domains.

The simulation and experimental results validate the easiness to tune the controller to achieve desired time response patterns, and its robustness in face of noisy uncertain bioreaction environments.

REFERENCES

- [1] G. Bastin and D. Dochain, *On-line Estimation and Adaptive Control of Bioreactors*. Elsevier, 1990.
- [2] H. De Battista, J. Picó, and E. Picó-Marco, "Nonlinear pi control of fed-batch processes for growth rate regulation," *Journal of Process Control*, vol. 22, no. 4, pp. 789–797, 4 2012.
- [3] K. S. Lee, P. Boccazzi, A. J. Sinskey, and R. J. Ram, "Microfluidic chemostat and turbidostat with flow rate, oxygen, and temperature control for dynamic continuous culture." *Lab Chip*, vol. 11, no. 10, pp. 1730–9, 5 2011.
- [4] C. N. Takahashi, A. W. Miller, F. Ekness, M. J. Dunham, and E. Klavins, "A low cost, customizable turbidostat for use in synthetic circuit characterization." *ACS Synth Biol*, 7 2014.
- [5] L. Mailleret, O. Bernard, and J.-P. P. Steyer, "Nonlinear adaptive control for bioreactors with unknown kinetics," *Automatica*, vol. 40, no. 8, pp. 1379–1385, 2004.
- [6] E. Picó-Marco, J. Picó*, and H. De Battista, "Sliding mode scheme for adaptive specific growth rate control in biotechnological fed-batch processes," *International Journal of Control*, vol. 78, no. 2, pp. 128–141, 2005.
- [7] H. De Battista, J. Picó, and E. Picó-Marco, "Globally stabilizing control of fed-batch processes with haldane kinetics using growth rate estimation feedback," *Journal of Process Control*, vol. 16, no. 8, pp. 865–875, 9 2006.
- [8] J. Picó, E. Picó-Marco, A. Vignoni, and H. De Battista, "Stability preserving maps for finite-time convergence: Super-twisting sliding-mode algorithm," *Automatica*, vol. 49, no. 2, pp. 534–539, 2 2013.
- [9] A. Vargas, J. A. Moreno, and A. Vande Wouwer, "A weighted variable gain super-twisting observer for the estimation of kinetic rates in biological systems," *Journal of Process Control*, vol. 24, no. 6, pp. 957–965, 6 2014.
- [10] H. De Battista, J. Picó, F. Garelli, and J. L. Navarro, "Reaction rate reconstruction from biomass concentration measurement in bioreactors using modified second-order sliding mode algorithms." *Bioprocess Biosyst Eng*, vol. 35, no. 9, pp. 1615–25, 11 2012.



Hernán De Battista received the M.S. and Ph.D. degrees in electronic engineering from the National University of La Plata (UNLP), La Plata, Argentina in 1994 and 2000 respectively. He is a research member of CONICET and a Full Professor at the Electrical Engineering Department, Faculty of Engineering of UNLP. His main research interests include nonlinear and switched control with applications to renewable energy and biological systems. He co-authored several books, as well as more than 40 journal papers.



Enric Picó-Marco received the M.S.Eng. and PhD degrees in control engineering from the Technical University of València (UPV) in 2000 and 2004 respectively. With a deep interest in mathematics, he has taken courses from the Open University, UK, degree of pure mathematics. He is also member of the American Mathematical Society. Entitled for Associate Professor, he is currently lecturer and researcher at the Department of Systems Engineering and Control, UPV. He has several journal papers and book chapters on control of bioreactors and nonlinear control. His current research interests include control of bioprocesses and alternatives to classic Lyapunov techniques to prove stability, specially in applications to general biological systems.



Fernando N. Santos-Navarro received the B.S. Eng. degree in electronic engineering from the Technical University of València in 2016. Currently he pursues a M.S. Eng. in control engineering as previous step towards a PhD. He has taken part in the iGEM competition on synthetic biology, where he won the prizes to the Best Software and Best Hardware with the project HypeIT in 2016. His interests are in synthetic biology, control of bioprocesses and low-cost hardware equipment.



Jesús Picó received the M.S.Eng. degree in engineering science and the Ph.D. degree in control engineering from the Technical University of València (UPV), Spain, in 1989 and 1996 respectively. Currently he is Full Professor at the Department of Systems Engineering and Control, UPV. He is member of the IFAC Technical Committee on Biosystems and Bioprocesses, and has published over 60 journal papers and book chapters on application of automatic control and multivariate statistic methodologies to bioprocesses control and estimation, and systems and synthetic biology. His current research interests include sliding mode observers and nonlinear adaptive control of bioreactors, control of protein expression and noise over populations of cells, control of cell gene synthetic circuits with metabolic burden constraints, and multiobjective optimization for analysis, synthesis and tuning gene synthetic circuits.

2 MÓDULO eQEP. MEDICIÓN DE FRECUENCIA

Para medir la frecuencia se ha utilizado el módulo eQEP de la BeagleBone Black. Este módulo es usado típicamente para medir la posición de encoders, llegando a medir frecuencias de 4MHz.

El módulo eQEP se carga con los siguientes comandos en la BeagleBone Black:

```
export SLOTS=/sys/devices/platform/bone_capemgr/slots
echo bone_eqep0 > $SLOTS
```

De esta forma se carga el eqep0. Los pines son asociados al eqep0 son los siguientes:

eQEPO	Pins
eQEP0A_in	P9_42B
eQEP0B_in	P9_27
eQEP0_index	P9_41B
eQEP0_strobe	P9_25

El único que se utilizará es el eQEP0A_in (P9_42), es al que se conectará la señal de frecuencia del sensor.

Es modulo está configurado para encoders, por tanto es necesario cambiar el modo de funcionamiento del módulo eQEP para poder medir frecuencia. Se muestra su configuración y cómo se realizan las medidas en el siguiente código de ejemplo.

```
#include "bbb-eqep.h"

int main (int argc, char const *argv[])
{
    struct timeval tv1, tv2;
    int eqep_num;
    uint32_t eqep_pos;

    eQEP eqep(0);
    eqep.positionCounterSourceSelection(2); // Cambio a modo leer frecuencia

    eqep.resetPositionCounter(); // Resetar el contador a 0
    usleep(1000000); // Esperar 1 segundo
    eqep_pos = eqep.getPosition()/2; // Por cada flanco se produce 1 tick. Hz

    return 0;
}
```

3 PROTOCOLO DE COMUNICACIÓN TCP CLIENTE-SERVIDOR

En el presente proyecto se ha implementado un protocolo de comunicación tipo cliente-servidor mediante TCP-IP.

Los mensajes se encuentran delimitados por saltos de línea ('\n'), y para indicar el fin de la transmisión de un fichero se utiliza el carácter '@'. Los mensajes pueden ser arbitrariamente grandes, pero se aconseja no superar los 1024 bytes por mensaje.

Se indicará a continuación los comandos implementados, los argumentos que se utilizan con ellos y la respuesta que devuelven.

- **help**

Devuelve un mensaje de bienvenida. En el futuro se implementará la ayuda

- **exit**

Cierra la comunicación con el servidor.

- **getState**

Devuelve el estado de la máquina de estados del turbidostato.

- **changeState (int) newState**

Cambia el estado de la máquina de estados del turbidostato al estado proporcionado. Devuelve el estado final del turbidostato, para comprobar que se ha realizado exitosamente el cambio.

- **getDt**

Devuelve el tiempo de muestreo en minutos.

- **setDt (float) newDt**

Fija el tiempo de muestreo al nuevo valor y después devuelve el tiempo de muestreo actual para comprobar que se ha realizado exitosamente el cambio.

- **getAllTSid**

Devuelve el id de todas las cámaras del turbidostato.

- **getODrefTS (int) id**

Devuelve la referencia de OD de la cámara de turbidostato de ese id.

- **setODrefTS (int) id (float) newODref**

Fija la referencia de OD de la cámara de turbidostato de ese id y después devuelve su valor para comprobar que se ha realizado exitosamente el cambio.

- **getSimTS (int) id**

Devuelve si se encuentra en estado simulación la cámara de turbidostato de ese id.

- **setSimTS (int) id (int) sim**

Cambia el estado simulación de la cámara de turbidostato de ese id y después devuelve el valor para comprobar que se ha realizado exitosamente el cambio.

- **getIsRunningTS (int) id**

Devuelve si se encuentra en marcha la cámara de turbidostato de ese id.

- **setIsRunningTS (int) id (int) sim**

Cambia el estado de funcionamiento de la cámara de turbidostato de ese id y después devuelve el valor para comprobar que se ha realizado exitosamente el cambio.

- **getDataTS (int) id**

Devuelve todos los datos del experimento asociado a la cámara de ese id como un fichero.

- **getControlNameTS (int) id**

Devuelve el nombre del controlador que se está usando en la cámara de ese id.

- **setControlNameTS (int) id (str) nameC**

Cambia el controlador que se está usando en la cámara de ese id y devuelve el nombre del controlador para comprobar que se ha realizado exitosamente el cambio.

- **getAllControlNameTS (int) id**

Devuelve una lista con el nombre de todos los controladores posibles para la cámara con ese id.

- **getAllParameterNameTS (int) id**

Devuelve una lista con el nombre de todos los parámetros modificables del controlador actual de ese id de cámara.

- **getAllParameterValuesTS (int) id**

Devuelve una lista con el valor de todos los parámetros modificables del controlador actual de ese id de cámara.

- **setAllParameterValuesT (int) id (double) value1 (double) value2 ...**

Cambia el valor de los parámetros del controlador de la cámara de ese id, y después devuelve una lista con todos los valores para comprobar que se ha realizado exitosamente el cambio.